

Imaging

713

ORAL

Prospective study of 18FDG-PET in patients with cervical lymph node metastases from an unknown primary tumor

J. Johansen^{1,7}, A. Eigved², S. Buus³, T. Bundgaard⁴, J. Marving², J. Kirkegaard⁵, S. Keiding³, M. Overgaard⁶, H.S. Hansen⁷. ¹Odense University Hospital, Dept. of Oncology, Odense, Denmark; ²Rigshospitalet, PET and Cyclotron Unit, Copenhagen, Denmark; ³Aarhus University Hospital, PET Center, Aarhus, Denmark; ⁴Aarhus University Hospital, Dept. of ENT, Aarhus, Denmark; ⁵Rigshospitalet, Dept. of ENT, Copenhagen, Denmark; ⁶Aarhus University Hospital, Dept. of Oncology, Aarhus, Denmark; ⁷Rigshospitalet, Dept. of Oncology, Copenhagen, Denmark, on behalf of DAHANCA;⁸

Background: Several retrospective studies have indicated that FDG-PET is a valuable diagnostic tool in the detection of a carcinoma of unknown primary (CUP) in patients with a metastatic neck lesion. We conducted a prospective study to investigate whether the previous PET results could be confirmed.

Material & Methods: A prospective study (DAHANCA-13) was set up by the Danish Head and Neck Cancer Group to include patients with cervical lymph node metastases from a squamous cell or undifferentiated CUP. The patients underwent conventional diagnostic work-up according to national guidelines including endoscopies, multiple mucosal biopsies and diagnostic CT/MR scans for image-fusion purposes. Subsequently, a whole-body 18F-FDG PET scan (281-534 MBq) was performed and pathological hot-spots were further investigated to confirm a primary tumor. 52 patients (38 men and 14 women) entered the study between January 2000 and December 2002.

Results: Focal pathological uptake indicated a primary tumor or metastatic disease in 50% of the patients (26/52); in 18 cases this was in the head and neck region, in 8 cases below the clavicles. Additional investigations confirmed a primary tumor in 14 of these patients: hypopharynx 4, oropharynx 3, nasopharynx 1, lung 1, axilla 1, bone 1, and multiple metastatic lesions 2. Unexpectedly, PET also detected a rectal tumor (adenocarcinoma). False positive PET scans were predominant in the oropharynx, presumably due to reactions after mucosal biopsies. Two false negative studies were observed (base of tongue, nasopharynx). In patients with a detected primary tumor or extensive metastatic disease, treatment was modified from the PET results according to the observed tumor extension towards targeted curative treatment or palliation, respectively.

Conclusions: This prospective study confirmed the efficacy of whole-body 18F-FDG PET in CUP patients by detecting either primary tumors or metastatic disease in 27% (14/52). PET findings allowed radiation treatment fields and fractionation schedules to be individually modified and, thus, PET had significant treatment-related implications.

714

ORAL

Hypoxia within human prostate cancer: a correlation of quantified BOLD MRI with pimonidazole immunohistochemistry

D.M. Carnell¹, N.J. Taylor², R.E. Smith³, J.J. Stirling², A.R. Padhani², P.J. Hoskin¹. ¹Marie Curie Research Wing, Mount Vernon Cancer Centre, Northwood, United Kingdom; ²Paul Strickland Scanner Centre, Mount Vernon Cancer Centre, Northwood, United Kingdom; ³Department of Histopathology, Mount Vernon Cancer Centre, Northwood, United Kingdom

Background: The spatial distribution of MRI parameters (unstimulated R2* & relative blood volume) is compared with pimonidazole stained prostatectomy sections to assess the ability of MRI to predict clinically significant prostate cancer hypoxia. This could potentially be used to localise an IMRT boost to radio-resistant hypoxic areas.

Material and methods: Following local ethical approval, 5 patients (age 53-69 yrs old; Gleason score, 6-7; serum PSA, 5.9-15 ng/ml) with localised prostate carcinoma were imaged prior to receiving 0.5g/m² pimonidazole intravenously 16-24 hours before radical prostatectomy. Patients were imaged in a Symphony 1.5T MRI scanner (Siemens, Germany) using a phased array pelvic coil. T₂-weighted images were used to stage tumours and to identify tumour slice locations (1 slice location per patient). Multiple gradient echo images were acquired with varying TE (5-75ms), TR=100ms, α=40°, FOV=200mm and 256² matrix from which R2* maps were calculated. A dynamic series of 60 GRE T2*-weighted images was then acquired (TE=20ms, TR=34ms, 64x128 matrix, α=40° and time resolution

2.01s) using 0.2mmol/kg body weight Gd-DTPA (Magnevist®, Schering Healthcare). A gamma variate fit function was applied to the data on a pixel-by-pixel basis and relative blood volume (rBV) maps were calculated. Images were segmented for areas of fast R2* (similar intensity to muscle) and areas of rBV greater than fat and mapped onto a prostate gland outline. Histological sections, stained with H&E for tumour localisation and with pimonidazole (hypoxia detection), obtained in the imaging plane, were inspected at low power (x4) and independently mapped on the same prostate gland outline. Correspondences between MRI metrics with histology were performed using 5x5mm grid overlays. The results were analysed using a 2x2 table analysis for regions predominantly containing tumour (>50% of a grid with tumour: 133 grid locations) and non-tumour prostatic tissues (165 grid locations).

Tissue type & criteria for MRI	Hypoxia prevalence %	Sens %	Spec %	PPV %	NPV %	LR+ve	LR-ve
Non-tumour (R2*+rBV)	25	50	56	28	77	1.1	0.9
Tumours (R2*+rBV)	63	78	62	78	62	2.1	0.4
Tumours (R2* alone)	63	96	59	80	89	2.3	0.1
Tumours (rBV alone)	63	80	3	59	9	0.8	5.8

Sens=sensitivity; Spec=specificity; PPV&NPV=positive&negative predictive values; LR=likelihood ratios of a positive and negative test.

Results: Hypoxia was found in benign prostatic hyperplasia. For tumour, 48/60 grids with fast R2* stained positive for pimonidazole and 17/19 grids with slow R2* stained negative. The results (Table) show that MRI is better able to identify hypoxia in tumours compared to non-tumour tissues. R2* alone best reflects the oxygenation status of tumours and adding rBV information reduced the sensitivity (96% to 78%) and NPV (89% to 62%) without improving specificity. On average a positive MRI result with R2* is twice as likely to indicate tumour hypoxia as not, but this does not hold true for normal tissues.

Conclusions: These early patient data provide evidence that unstimulated BOLD-MRI allows non-invasive mapping of significant hypoxia within human prostate cancer. A larger cohort of patient is currently being analysed to verify these findings.

715

ORAL

Biodistribution of radiolabelled liposomal doxorubicin in mice by scintigraphic imaging

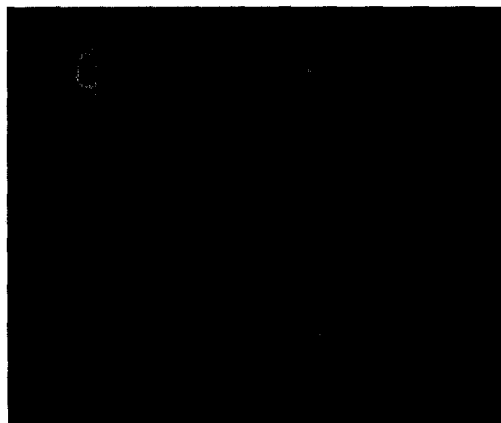
M. Frier¹, S.H. Yong², A.C. Perkins², M. Garnett², P. Daza-Ramirez³. ¹Queen's Medical Centre Nottingham, Radiopharmacy Unit, Dept of Medical Physics, Nottingham, United Kingdom; ²University of Nottingham, Nottingham, United Kingdom; ³Elan Pharma Ltd, Stevenage, United Kingdom

Background: Pharmaceutical formulations are designed to optimise drug delivery to improve efficacy and reduce side effects. Demonstrating these benefits by clinical outcomes can be difficult, subjective and demanding in terms of resources. The same benefits can be demonstrated directly by visualisation of biodistribution, but attachment of markers to the delivery system requires careful validation. Liposomal systems containing radioactive tracers have been widely studied using gamma scintigraphy. Most studies have used liposomes containing ligands incorporating the radiotracer, and few have studied commercially available therapeutic formulations. Our study describes the labelling, characterisation and biodistribution of a non-pegylated liposomal formulation of doxorubicin (Myocet®).

Materials & Methods: Liposomes were labelled using the lipophilic tracer ^{99m}Tc exametazime (Cereteq®) and incubated with stannous chloride to fix activity. Doxorubicin was loaded into the liposomes via a pH gradient. The method was validated in preparation for a human study. Leakage of doxorubicin from the liposomes was assessed in saline suspension and in the presence of plasma by fluorescence spectrometry. Biodistribution studies were performed in MCF7 xenografted mice (n=4), with serial images at intervals up to 24 h post-injection. Animals were sacrificed at 24 h and organs removed for radioactivity counting.

Results: The method produced high (>95%) labelling efficiency with high stability and low drug leakage. Zeta potential and particle sizing studies demonstrated no significant differences from unlabelled product. Accumulation of ^{99m}Tc-labelled liposomes was observed in spleen, stomach, liver, kidney, tumour and lungs. The image shows timecourse of biodistribution of ^{99m}Tc-labelled liposomes in an MCF7 xenografted mouse (xenograft implanted in left flank) shown by series of gamma-camera pictures. Tumour:blood ratio of radioactivity at 24 h was 7.1:1. Myocardium:blood at the same time was 0.8:1.

Conclusions: The radiolabelling procedure enables the study of biodistribution of a preformed liposomal formulation. The method is applicable to



studies in humans, and a study in patients is ongoing. The data support observations of improved efficacy and reduced cardiotoxicity using this method of drug delivery, and suggest that in clinical use in metastatic breast cancer patients the liposomal formulation will provide an enhanced therapeutic index compared with conventional doxorubicin.

716

ORAL

Detection and characterisation of novel biliary metabolites of the anticancer agent ifosfamide using in-vivo and analytical ^{31}P MRS and mass spectrometry

G.S. Payne¹, A.S.K. Dzik-Jurasz¹, L. Mancini¹, B. Nutley², F. Raynaud², M.O. Leach¹, ¹Royal Marsden Hosp & Institute of Cancer Research, Cancer Research UK Clin Magnetic Resonance Group, SUTTON, United Kingdom; ²The Institute of Cancer Research, Cancer Research UK Centre for Cancer Therapeutics, SUTTON, United Kingdom

Introduction: Many drugs undergo biliary excretion, potentially affecting pharmacokinetics and toxicology. Conventional methods to study this are highly invasive. Here biliary excretion of metabolites of the alkylating agent ifosfamide (IF) is demonstrated using *in vivo* ^{31}P Magnetic Resonance Spectroscopy (MRS). High resolution ^{31}P -MRS and analytical mass spectrometry enabled provisional assignment of the major biliary metabolite to the glutathione conjugate of IF. The conjugate represents a previously unreported metabolite of IF.

In vivo studies: Ten male Dunkin-Hartley guinea pigs (900 ± 20 g) were cannulated, anaesthetised and placed prone over a $5\text{cm } ^1\text{H}/^{31}\text{P}$ coil system¹ in a 1.5T Siemens Vision MR scanner. A peak at the IF frequency appears within 20 minutes of administration of 500mg/kg IF (Fig 1). Localised data (Fig 2) show that IF signal arises from the liver and gall bladder.

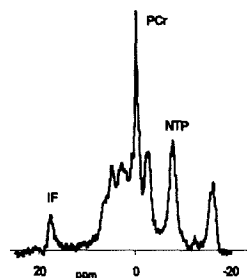


Fig. 1. Unlocalised ^{31}P MRS in vivo after 500 mg/kg IF

High Field ^{31}P MRS Studies of Bile: Spectra of extracted bile were acquired at 11.74 T (Fig 3). Spiking identified Peak 5 as IF. Published data from measurements in urine² suggest Peak 2 is carboxy IF, while Peak 3 is 2-dechloroethyl IF or 2,3-dechloroethyl IF. Peak 4 has not previously been reported. If gall bladder volume is 4 cm^3 then approximately 1.9% of injected IF is present as IF and its metabolites in the bile.

Identification of the 16.02 ppm peak using Liquid Chromatography Mass Spectrometry (LCMS): LC analytes were ionised and their masses measured using an ion trap mass spectrometer. The most intense peak detected not present in control bile had a molecular weight of 531, consistent with formation of a conjugate of IF where one Cl atom has been replaced with GSH. Comparative MSMS fragmentation of GSH, IF and the putative GS-IF conjugate showed patterns consistent with this.

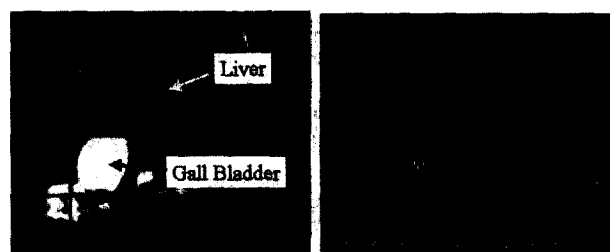


Fig 2. CSI-localised ^1H -decoupled ^{31}P MR Spectra from guinea pig following administration of 500 mg/kg IF

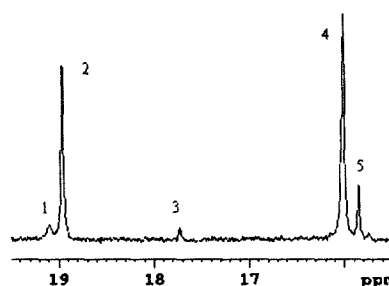


Fig 3. ^{31}P MR Spectrum from Bile at 11.74 T

Table 1. Metabolite concentrations in bile (N=10; mean \pm s.d.)

Peak	ppm	Conc (mM)
1	19.09	0.49 ± 0.25
2	18.96	2.04 ± 1.04
3	17.74	0.16 ± 0.07
4	16.02	4.05 ± 2.38
5	15.86	1.19 ± 1.47

Conclusions: ^{31}P MRS signals *in vivo* of IF and its metabolites arise predominantly from liver and gall bladder. Biliary excretion of IF or its metabolites has not previously been reported. High-resolution ^{31}P MRS and mass spectrometry show the main metabolite present to be GSH conjugate of IF. These or other biliary metabolites may be implicated in previously described oxazophosphorine related cholecystitis³⁻⁵.

Acknowledgements: This work was funded by Cancer Research UK (C1060/A808/G7643)

References

- [1] DWJ Klomp. Magn. Reson. Imag. 19: 755 (2001).
- [2] R Martino. J Pharmacol. Exp. Ther. 260: 1133 (1992).
- [3] CR Swanepoel Br Med J. 286: 251.
- [4] C Collins. Cancer 63: 228 (1989)
- [5] Kuttah Ann Oncol. 6: 302 (1995).

Paediatric oncology

717

ORAL

Risk adapted treatment for childhood hepatoblastoma (HB): final report of the second study of the International Society of Paediatric Oncology' SIOPEL 2

G. Perilongo¹, E. Shafford², L. Brugieres³, P. Brook⁴, R. Maibach⁵, P. Czauderna⁶, G. Mackinlay⁷, D. Arosen⁸, M. Childs⁹, J. Plaschkes¹⁰. ¹Division of Haematology-Oncology, Department of Pediatrics, Padova, Italy; ²Pediatric Oncology Unit, St. Bartholomew's Hospital, London, United Kingdom; ³Service d'Oncologie Pédiatrique, Institut Gustave Roussy, Paris, France; ⁴Paediatric Oncology Unit, The Hospital for Sick Children, London, United Kingdom; ⁵Department of Pediatric Surgery, Medical University, Gdansk, Poland; ⁶Pediatric Surgical Unit, Royal Hospital for Sick Children, Edinburgh, United Kingdom; ⁷Pediatric Surgical Unit, AMC, Amsterdam, The Netherlands; ⁸Pediatric Surgical Unit, Children's Hospital, Berne, Switzerland

Background: SIOPEL2 was a co-operative, international pilot study aiming to test effectiveness - in terms of response, resection rate (RR, RsR), progression-free (PFS), overall survival (OS) - and toxicity of two chemotherapy regimens, incorporated into a therapeutic strategy based on